Headgroup Motion in a Lyotropic Lamellar Phase by Deuterium and Nitrogen-14 Relaxation Studies

Ronald Y. Dong*,†,‡ and Yanbin Chen‡

Department of Physics and Astronomy, Brandon University, Brandon, MB, Canada R7A 6A9, and Department of Physics and Astronomy, University of Manitoba, Winnipeg, MB, Canada R3T 2N2

Received: July 6, 2005; In Final Form: August 31, 2005

Deuterium (^{2}H) and nitrogen-14 (^{14}N) NMR spectroscopy were used to investigate the molecular dynamics of a lyotropic liquid crystal. Deuterium spectral densities of motion for the C_1 deuterated site on the chain of the molecule decylammonium chloride (DACl) at the Larmor frequency 61.4 MHz and those for the ^{14}N at the headgroup (NH_3^+) at 28.9 MHz are analyzed quantitatively in the lamellar phase of the DACl-d_{11}/water binary system to shed light on the headgroup dynamics. The motional model used is the small step rotational diffusion for reorientations plus internal rotations of the methylene group in the strong collision limit. The tumbling motion of the long axis of the DACl molecule in the aggregates seems to be as rigorous as the molecular spinning motion, likely due to the proposed motional model. The similarity of deuterium spectral densities from the C_1 and C_2/C_3 sites may indicate a relatively rigid unit of $C_1-C_2-C_3$ in the backbone.

1. Introduction

Lyotropic liquid crystals[1] present some interesting self-assembling phases, which may not be found in thermotropic counterparts. In particular, the decylammonium chloride (DACl)/H_2O binary system has been popular as a model system in the study of lyotropic liquid crystals[2,3] and biological membranes. It belongs to a family of long-chain cationic surfactants, whose structures differ by the number of carbons and the type of halides.[4,5] In higher DACl concentrations, a variety of mesophases can be created, including hexagonal phase, lamellar phase, and micellar isotropic phase.[6] Using ^{1}H NMR fast field cycling T_1 measurements, Wachowicz et al.[2] recently found that layer undulations (or ODF) make an important contribution to slow molecular dynamics with a characteristic frequency dependence in the lamellar phase. This indicates a relatively weak interaction between neighboring decylammonium chloride layers in water. But in the high-frequency region ($>10^5$ Hz), fast molecular motions[7] are found to dominate the dynamics in the hexagonal phase of a dodecylammonium chloride/H_2O system. These include rotation of alkyl chains about their long molecular axes, trans-gauche isomerization, and lateral self-diffusion. In consideration of fast local reorientations and surface diffusion of molecules around the aggregate axes, Halle's group[8] proposed a motion model for spin relaxation in the hexagonal phase, which was successfully applied by one of us[9] to interpret the ^{14}N relaxation measurements in a similar binary system. NMR study of the micellar phase in the DACl/H_2O system has also been reported.[2] However, the study of lamellar phase in lyotropics is still rare. Here we present the spin−lattice relaxation data in the lamellar phase of DACl/H_2O by exploiting both ^{2}H and ^{14}N nuclei. It is noted that NQR has been reported in the crystalline phase of DACl.[10] In particular, the ^{14}N quadrupolar coupling constant has been determined as 760 kHz in this solid. Despite its low gyromagnetic ratio and difficulty in detection, the ^{14}N spectrum is easily identified and less affected by liquid crystal impurities.[11] Partially deuterated DACl samples are labeled in the first three alkyl carbon sites and the last methylene and methyl groups. These samples have also been studied by ^{2}H NMR in its solid phases.[12] The aim of this work is to use deuterons on the first three alkyl carbon sites of DACl and the nitrogen on its headgroup to study their relaxation properties in order to understand the overall molecular motion in the lamellar phase.

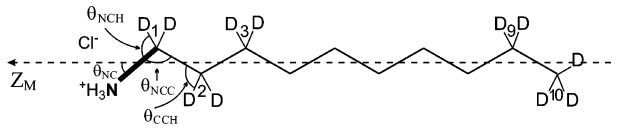

Figure 1. Schematic structure of the partially deuterated DACl molecule at carbon sites C_1, C_2/C_3, C_9, and C_{10} in its all-trans configuration. The angles are used in the superimposed rotations model, while the dashed line is the long molecular Z_M axis.

2. Experimental Section

A. NMR Samples. The DACl crystal was synthesized by C. Morcombe, Brandon University. Selectively deuterated 1,9,10-DACl-d_7 and 2,3-DACl-d_4 samples were provided by Dr. A. S. Tracey, Simon Fraser University. Two nondeuterated DACl/H_2O (54 wt %) and DACl/H_2O (56 wt %) samples were packed into 7.5 mm NMR tubes. The two deuterated DACl crystals were mixed to a weight ratio of 2 to 1, then used as the solute 1,2,3,9,10-DACl-d_{11} to mix with doubly distilled water, giving samples of different concentrations. The DACl/D_2O binary system was prepared at a range of concentrations (38−59wt %) in NMR tubes for mapping the phase diagram and ^{14}N study, while the deuterated DACl/H_2O binary system of several concentrations was used for ^{2}H relaxation study. The method and procedures in preparing DACl/H_2O samples have been detailed eslewhere.[13] The uncertainties in sample concentrations were estimated as less than 2%.

^{2}H NMR investigation was focused on a series of samples with concentration chosen to cover the interested region of the DACl/H_2O phase diagram.[6] Here we report results from 54 and

† Brandon University.
‡ University of Manitoba.

10.1021/jp053694c CCC: $30.25
Published on Web 09/29/2005

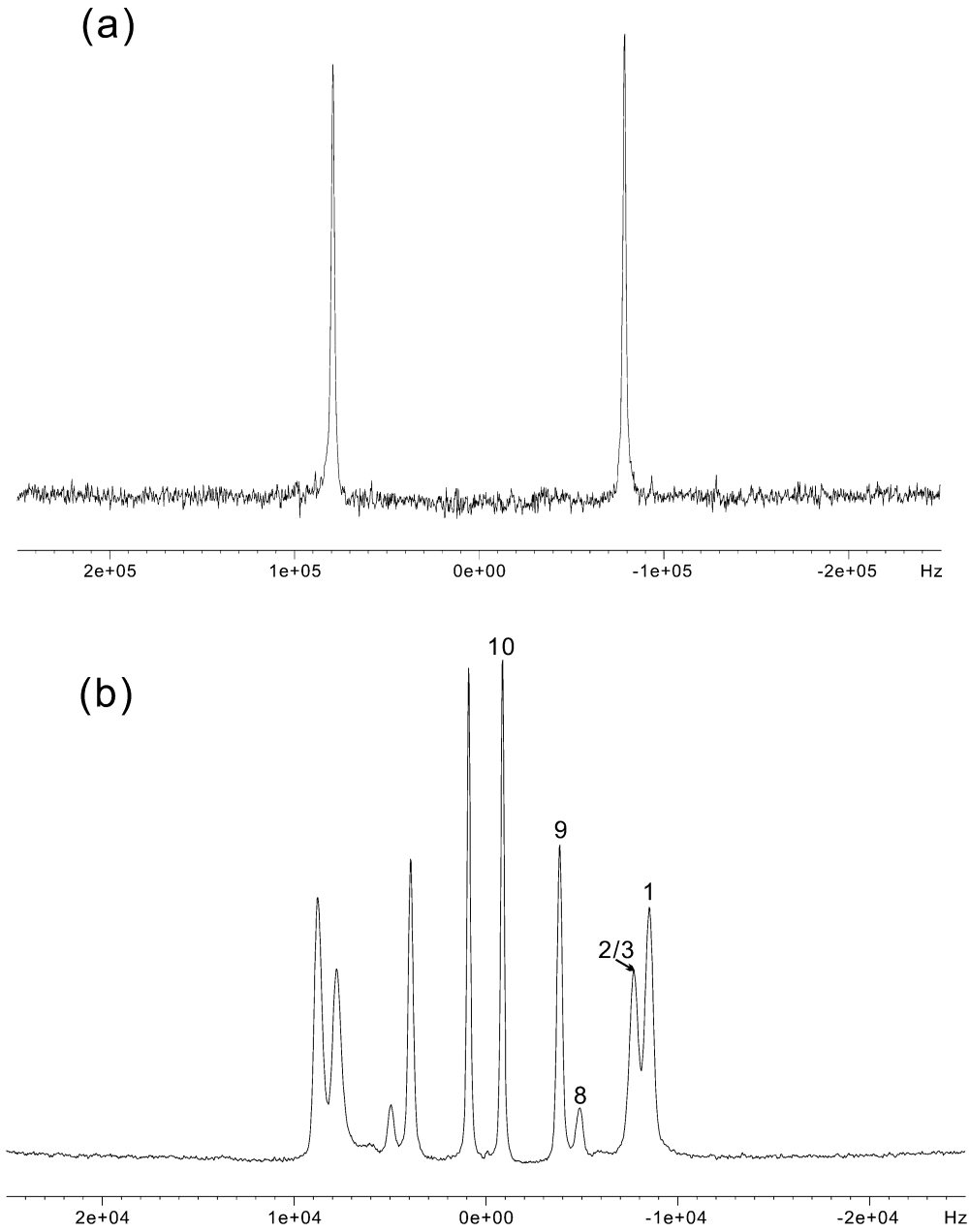

Figure 2. A typical nitrogen-14 NMR spectrum (303.5 K) of 56 wt % DACl/H_2O sample (a) and a typical deuterium spectrum (323 K) with peak assignments of 54 wt % DACl/H_2O sample (b). Note that the noise is much greater in Figure 2a.

56 wt % of 1,2,3,9,10-DACl-d_{11} in H_2O to study their lamellar phase. 1,9,10-DACl-d_7 and 2,3-DACl-d_4 were also mixed respectively with water, and both were at 54 wt % for spectral reference. By measuring a sample containing only one kind of selectively deuterated material,[12] it was found that the C_2, C_3 doublets appear indistinguishable, thereby only one quadrupolar splitting and its corresponding spin−lattice relaxation times could be recorded. On the other hand, in the lamellar phase of 1,9,10-DACl-d_7/H_2O, besides the $\Delta\nu_1$, $\Delta\nu_9$, and $\Delta\nu_{10}$, there appeared an additional weak splitting, which arises probably from an accidentally deuterated carbon site. It is tentatively assigned for C_8, based on the observed splitting of C_7 reported before.[2] Thus in total, there are five doublets in the combined deuterated lyotropic samples (Figure 2b).

The samples were usually not well aligned when first cooled from the isotropic phase into the lamellar phase. The sample was heated again and allowed to stay at some high temperature for a few hours before being cooled down slowly. This kind of process might be repeated several times until a well-aligned sample was finally achieved. The deuterated 54 wt % DACl sample was heated to 345 K to give the micellar isotropic phase, while the deuterated 56 wt % one was heated to 360 K. Before completely turning into isotropic, a lamellar-isotropic biphasic region extending ca. 10−20 deg appears, which is consistent with the phase diagram reported earlier[6] by polarizing microscopy detection. In our case, the boundary of the biphasic region was actually determined by the onset of relatively temperature-insensitive C_1 (and ^{14}N) splittings and the existence of an isotropic peak between the doublets in the spectrum. In fact, this isotropic peak exists for quite a wide temperature range even into the lamellar phase. The phase transition temperatures of our samples are summarized in Table 1.

B. Deuterium and Nitrogen-14 NMR. The experiments were performed with a Bruker Avance 400 spectrometer and a 9.4 T superconducting magnet. The sample temperature was regulated by an air flow to better than 0.1 °C. The deuterium NMR measurements were performed with a Bruker PE probe, having a coil diameter of 5 mm. The samples were sealed in 4 mm

TABLE 1: Transition Temperatures for the Samples Used in Both ^{2}H and ^{14}N Studies

sample wt %	phases and transition temperatures
54	lamellar $\xrightarrow{334\ K}$ lamellar + isotropic $\xrightarrow{345\ K}$ isotropic
56	lamellar $\xrightarrow{342\ K}$ lamellar + isotropic $\xrightarrow{357\ K}$ isotropic

NMR tubes to save the amount of deuterated materials. The 90° pulse width was usually 3.4 μs. Typically, 32 accumulations were used to improve the signal-to-noise (S/N) ratio of resulting spectra. The broadband version of the Jeener−Broekaert sequence[14] was used to measure the spin−lattice relaxation times of the Zeeman (T_{1Z}) and quadrupolar (T_{1Q}) order simultaneously. The time between the first and the second pulse was between 8 and 20 μs depending on doublets of interest and the temperature. The relaxation times of the five doublets vary widely, ranging from 50 ms for ^{2}H at the carbon C_1 site (near the headgroup) to over 1 s for ^{2}H at the carbon C_{10} (at the end of the chain). The observation is, however, different from those reported previously[2] for the C_2 and C_7 sites of DACl.

For ^{14}N study at 28.9 MHz, a modified Bruker probe with a coil diameter of 7.5 mm was used to accommodate larger sample sizes because of S/N consideration. A 90° pulse width between 3.7 and 3.9 μs was employed. In fact, to measure the extraordinarily large splitting of the ^{14}N doublet, which is between 120 and 160 kHz (not shown here), a shorter pulse width should be employed, but such amount of rf energy tends to cause arching in the probe. Signal averaging of 16 000 scans was routine in the literature,[9,11] while here the number of scans was up to 8 000 to obtain good spectra. Again T_{1Z} and T_{1Q} relaxation times were measured by the broadband Jeener−Broekaert sequence. Pulse separation between the first and second pulse of 5 to 20 μs was used at different temperatures according to the ^{14}N splitting. At lower temperature, a pulse separation of less than 4 μs was found to give a slightly better broadband irradiation. The accuracy in T_{1Z} and T_{1Q} measurements is estimated at about 8% and less than 5% for the ^{14}N and ^{2}H case, respectively.

3. Theory

A schematic diagram of the DACl molecule is shown in Figure 1. In the lamellar phase, the location of the long molecular Z_M axis for DACl is still unknown. However, in the crystalline phase C_2 to C_{10} backbone on the DACl chain is supposed to be coplanar, while N and C_1 are displaced significantly from these ideal carbon zigzag planes.[4,5] The failure of placing the N−C_1 bond on the Z_M axis in our spectral density simulations seems to confirm a non-zero θ_{NC} angle between the N−C_1 bond and the long Z_M axis. This angle was estimated to be about 30° in a recent NQR study.[10] From our simulations of the C_1 $^2H_{C1}$ and ^{14}N spectral densities, θ_{NC} of 26° and 28° produced satisfactory results for 56 and 54 wt % DACl/H_2O, respectively. However, the uncertainty in the magnitude of θ_{NC} could be 3° if taking experimental errors into account.[13]

A typical ^{14}N NMR spectrum (Figure 2a) was similar to the deuterium spectrum (Figure 2b). From the quadrupolar splittings of ^{2}H NMR spectra, segmental order parameters $S_{CD}^{(i)}$ of the C_i−D bond can be obtained with eq 1. In the aligned lamellar phase, the layer normal is perpendicular to the magnetic field, and the symmetry axis of the aggregate is along the layer normal giving[2,15]

$$\Delta\nu_i = \frac{3}{4} q_{CD} S_{CD}^{(i)} \qquad (1)$$

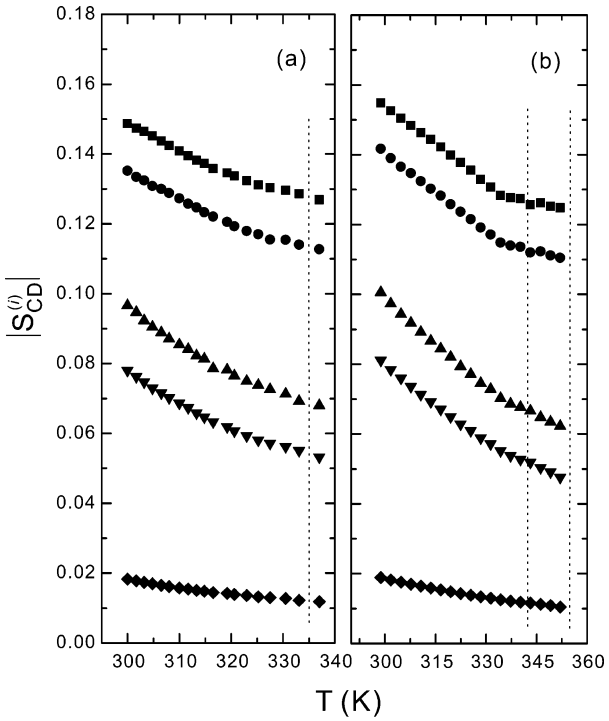

Figure 3. Temperature dependence of segmental order parameters of C_1 (squares), C_2/C_3 (circles), C_8 (up triangles), C_9 (down triangles), and C_{10} (diamonds) deuterons for 54 (a) and 56 wt % (b) of DACl in H_2O. In part a, to the right of the dotted line shows the biphasic region. In part b, the region between the dotted lines is the biphasic region, and that to its right is the isotropic micellar phase.

where q_{CD} is the quadrupolar coupling constant for the methylene deuterons. The absolute S_{CD} values are shown in Figure 3 for the two studied partially deuterated DACl/H_2O samples. Applying eq 1 to ^{14}N, one obtains

$$\Delta\nu_N = \frac{3}{4} q_N S_{CN} = \frac{3}{4} q_N S_{zz} P_2(\cos\theta_{NC}) \qquad (2)$$

where q_N is the quadrupolar coupling constant for nitrogen, S_{CN} refers to the segmental order parameter of the C−N bond, and S_{zz} is the nematic order parameter. Similarly for $^2H_{C1}$ on the first carbon site,

$$\Delta\nu^{(1)} = \frac{3}{4} q_{CD} S_{CD} = \frac{3}{4} q_{CD} S_{zz} P_2(\cos\theta_{NC}) P_2(\cos\theta_{NCH}) \qquad (3)$$

where the ∠N−C_1−H (θ_{NCH}) =106.7° is used, and q_{CD} is taken to be 170 kHz.[16] Combining eqs 2 and 3 and using the ^{2}H and ^{14}N splitting at each temperature yields the value of q_N. q_N was found to change weakly with temperature. Thus, it was taken to be the average value, 523.2 kHz for the 56 wt % DACl/H_2O sample and 503.5 kHz for the 54 wt % sample in the subsequent spectral density calculations. These q_N values in the lamellar phase are similar to (but lower than) the value obtained in crystal.[10]

The spectral densities $J_1(\omega_0,\Theta)$ and $J_2(2\omega_0,\Theta)$ are derived from the spin−lattice relaxation times according to:

$$\frac{1}{T_{1Q}} = 3J_1(\omega_0,\Theta) \qquad (4)$$

$$\frac{1}{T_{1Z}} J_1(\omega_0,\Theta) + 4J_2(2\omega_0,\Theta) \quad (5)$$

where $\omega_0/2\pi$ is the Larmor frequency, and Θ (=90°) is the angle between the external magnetic field and the phase director (planar normal) in the lamellar phase. The spectral densities measured at $\Theta = 90°$ can be related to the spectral densities $J_m(\omega,0°)$ for $\Theta = 0°$ in a simplified form according to[17−19]

$$J_1(\omega,90°) = \frac{1}{2}[J_1(\omega,0°) + J_2(\omega,0°)] \quad (6)$$

$$J_2(2\omega,90°) = \frac{3}{8}J_0(2\omega,0°) + \frac{1}{2}(2\omega,0°) + \frac{1}{8}J_2(2\omega,0°) \quad (7)$$

It is worth noting that lamellar phase is uniaxial. Taking into account the superposition of different kinds of motion, such as collective director fluctuations, molecular rotations, and internal isomerization, these spectral densities can be calculated by a suitable model. Collective fluctuations of layers are relatively unimportant[7] at frequencies above 10 MHz, and a small step rotation diffusion model[20,21] is adopted to describe the molecular reorientation of the DACl molecule. The rotational diffusion equation solved by Tarroni and Zannoni[21] is now applied. Superimposed bond rotations on the overall motion with the strong collision limit[22] are employed to account for the internal rotation of the first methylene group.

The spectral densities for the nitrogen on the headgroup, labeled by a superscript N, are given for the director along the external field by

$$J_m^{N}(m\omega,0°) = \frac{3\pi^2}{2}(q_N)^2\sum_n [d_{n,0}{}^2(\theta_{NC})]^2 \times \sum_k \frac{(\beta_{mn}{}^2)_k(\alpha_{mn}{}^2)_k}{(m\omega)^2 + (\alpha_{mn}{}^2)_k{}^2} \quad (8)$$

where $d_{n,p}{}^2(\theta)$ is the Wigner matrix, the decay constants, $(\alpha_{mn}{}^2)_k/D_\perp$, are the eigenvalues of the rotational diffusion matrix, and $(\beta_{mn}{}^2)_k$, the corresponding eigenvectors, govern the relative weights of the exponentials in the correlation functions. Both diffusion coefficients $D_\perp$ and $D_\parallel$ appear in $(\alpha_{mn}{}^2)_k$, where $D_\perp$ represents the tumbling motion of the molecule about one of its short molecular axes, while $D_\parallel$ is the spinning motion about the long Z_M axis. For the deuterons ($^2H_{C1}$) on the chain C_1 site of DACl, methylene rotations are superimposed onto the reorientation to give

$$J_m^{^2H_C}(m\omega,0°) = \frac{3\pi^2}{2}(q_{CD})^2\sum_n\sum_p [d_{p,0}{}^2(\theta_{NCH})^2][d_{n,p}{}^2(\theta_{NC})]^2 \times \sum_k \frac{(\beta_{m,n}{}^2)_k[(\alpha_{mn}{}^2)_k + (1-\delta_{p,0})D']}{(m\omega)^2 + [(\alpha_{mn}{}^2)_k + (1-\delta_{p,0})D']^2} \quad (9)$$

where in the strong collision limit $\delta_{p,0}$ is the Kronecker delta function, and the diffusion coefficient D' is for the methylene bond rotation. Again using the superimposed rotations model,[22] the deuterons on the C_2 site give the following spectral densities

$$J_m^{^2H_C}(m\omega,0°) = \frac{3\pi^2}{2}(q_{CD})^2\sum_n\sum_j\sum_p [d_{p,0}{}^2(\theta_{CCH})]^2 \times [d_{j,p}{}^2(\theta_{NCC})]^2[d_{n,j}{}^2(\theta_{NC})]^2 \times \sum_k \frac{(\beta_{mn}{}^2)_k[(\alpha_{mn}{}^2)_k + (1-\delta_{j,0})D' + (1-\delta_{p,0})D'']}{(m\omega)^2 + [(\alpha_{mn}{}^2)_k + (1-\delta_{j,0})D' + (1-\delta_{p,0})D'']^2} \quad (10)$$

where D'' is the diffusion coefficient for the methylene deuterons rotating about the C_1-C_2 bond, $d_{j,p}{}^2(\theta_{NCC})$ denotes the Wigner matrix involved in the coordinate transformation from the C_1-C_2 segment to the $N-C_1$ bond, θ_{NCC} is assumed to equal the ∠C−C−C of 113.5°, and $\theta_{CCH} = 107.5°$ is used for the ∠C_1-C_2-H angle.[23,24]

4. Results and Discussion

^2H NMR spectra of selectively deuterated DACl molecules give information about fast anisotropic motions of a particular C−D bond. As seen in Figure 3, the segmental order parameters $S_{CD}^{(i)}$ (<0.18) as well as the small difference (<15%) among the two concentrations correspond to those reported by Wachowicz et al.[2] The smaller quadrupolar splitting and consequently the segmental order parameter S_{CD} observed for deuterons further down the carbon−carbon backbone reflect an increase in motional disorder along the chain. This is a consequence of an increase in gauche conformation probability.[3] Using eq 3 and the θ_{NC} value (26° or 28°), the orientational order parameter S_{zz} varies between 0.45 and 0.57 for the aligned DACl molecules in 54 ($\theta_{NC} = 28°$) and 56 wt % ($\theta_{NC} = 26°$) samples (Figure 4). In fact, S_{zz} and θ_{NC} were determined from the splittings in conjunction with the fitting of the spectral densities. The decrease in S_{zz} reflects an increase of disorder as the micellar phase is approached. The slightly higher order in 56 wt % than in 54 wt % DACl/H_2O system is due to an increase of the DACl concentration, and the increased viscosity in the sample.

Deuteron spectral densities $J_m(m\omega_0,90°)$ for methylene sites as a function of temperature in the lamellar phase are plotted in Figure 5 for the two deuterated samples (54 and 56 wt %). At a glance, crossovers between deuteron J_1 and J_2 are pronounced at the C_1 and C_2/C_3 sites, in both concentrations. This crossover phenomenon is quite rare among thermotropic liquid crystals[25] and has only been observed in a recent work.[26] In addition, spectral densities for C_1 and C_2/C_3 are the same within experimental error limits. Figures 6 and 7 show plots of ^{14}N and $^2H_{C1}$ spectral densities for 54 and 56 wt % DACl/H_2O samples, respectively. There is no obvious crossover in ^{14}N data in view of larger uncertainties of these data. That the two concentrations show similar temperature behaviors seems to enforce the validity of our ^{14}N results. Using eqs 6−9, we can simulate the smoothed spectral density data in the lamellar phase via a "global target" approach, in which an Arrhenius behavior is assumed for the various diffusion coefficients. Thus, the temperature dependence can be written as $D_i = D_i^\infty \exp[-E_a^i/RT]$, where i denotes the specific type of motion and E_a^i is the corresponding activation energy. As the geometry of the DACl structure in the lamellar phase is not fully known, θ_{NC} is first guessed by trial and error. The order parameter S_{zz} and the quadrupolar coupling constant q_N are then calculated by fitting both the splitting data of $^2H_{C1}$ and ^{14}N. After several simulations with an averaged q_N value, θ_{NC} is determined by the best fitting quality of ^{14}N and ^2H spectral densities. In the global approach, instead of fitting D_i^∞, the diffusion coefficients at some particular temperature T, D_{iT} were used. However, before running

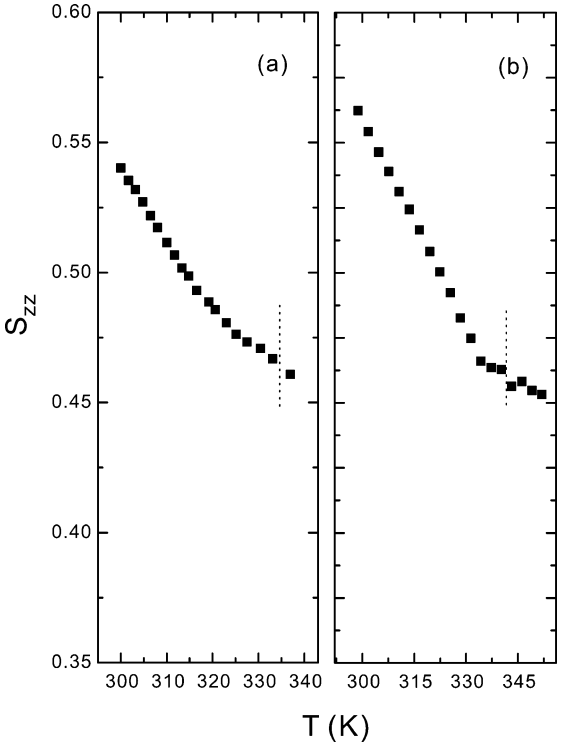

Figure 4. Temperature dependence of the nematic order parameter S_{zz} for a 54 (a) and 56 wt % (b) DACl/H_2O sample. The dotted line denotes the transition to the biphasic region.

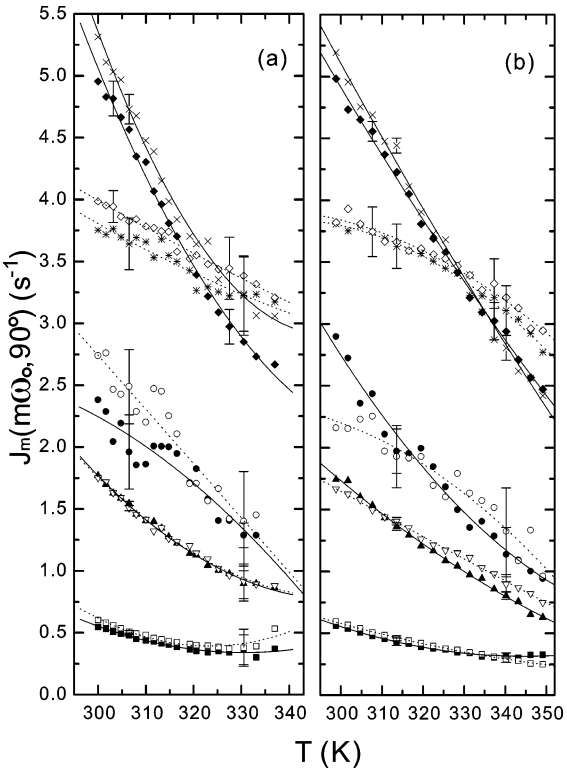

Figure 5. Plot of deuterium spectral densities of C_1 (diamonds), C_2/C_3 (crosses), C_8 (circles), C_9 (triangles), and C_{10} (squares) deuterons for the 54 (a) and 56 wt % (b) DACl in water. The closed symbols denote J_1, while the open symbols are for the corresponding J_2, except C_2 is denoted by $\times$. The solid (J_1) and dotted (J_2) curves are simply used to aid the eyes.

global target analysis a "single temperature" fitting facilitates the estimation of approximate target parameter values. At each temperature, four spectral densities determine three parameters

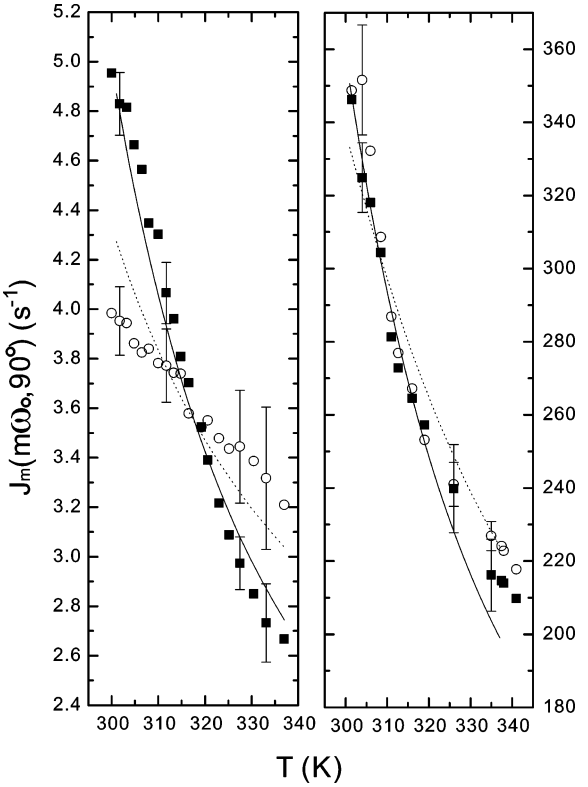

Figure 6. Plots of spectral densities of both $^2H_{C1}$ (left) and ^{14}N (right) of 54 wt % DACl in water. The closed squares and open circles refer to J_1 and J_2, respectively. Solid and dotted lines denote the corresponding calculated J_1 and J_2, respectively.

D', $D_{||}$, and $D_\perp$. For the global target analysis, the sum square fractional error f given by eq 11 is minimized by using AMOEBA[27]

$$f = \sum_k \sum_i \sum_m \frac{[J_m^{(i)\mathrm{Cal}}(m\omega) - J_m^{(i)\mathrm{Exp}}(m\omega)]_k^2}{[J_m^{(i)\mathrm{Exp}}(m\omega)]_k^2} \qquad (11)$$

where the sum over k is for 16 temperatures, the sum over i covers sites "^{14}N", "$^2H_{C1}$", and $m = 1$ and 2 (^{14}N at 28.9 MHz, and ^2H at 61.4 MHz). In total, 64 spectral densities were used to obtain 6 model parameters.

Calculated spectral densities from the global analysis at 28.9 and 61.4 MHz are shown as curves (solid lines for J_1, while dotted lines for J_2) in Figures 6 and 7. As seen in these diagrams, the fitting quality for both nuclei is fairly reasonable (e.g., $f =$ 0.08 and the crossover for C_1 deuterons is reproduced in the 54 wt % sample). As a consequence, the derived motional parameters shown in Figure 8 should be quite reliable, within the limitations of the proposed motional model. Table 2 summarizes the results for rotational diffusion coefficients and their activation energies. The error limits are estimated by varying one parameter while fixing the rest to their best values to yield a doubling in f value. It is noted that the tumbling motion is comparable to the spinning motion. This appears unrealistic, since the molecules are anchored at the interfacial water layers. The apparently fast tumbling diffusive motion of the long molecular axis may partly reflect the usual difficulty in getting reliable $D_\perp$ values as found in most thermotropics.[28] Nevertheless, the activation energy for the spinning motion is lower than that for the tumbling motion. This seems reasonable since DACl molecules are easy to rotate about the planar normal as they are loosely anchored on the water interfacial surface. However,

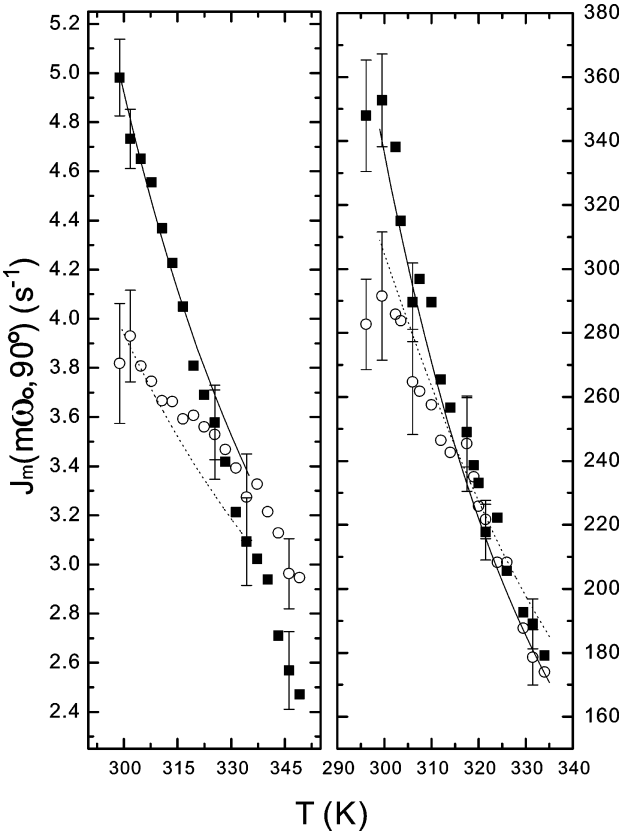

Figure 7. Plots of spectral densities of both $^2H_{C1}$ (left) and ^{14}N (right) of 56 wt % DACl in water. The closed squares and open circles refer to J_1 and J_2, respectively. Solid and dotted lines are the corresponding calculated value J_1 and J_2, respectively.

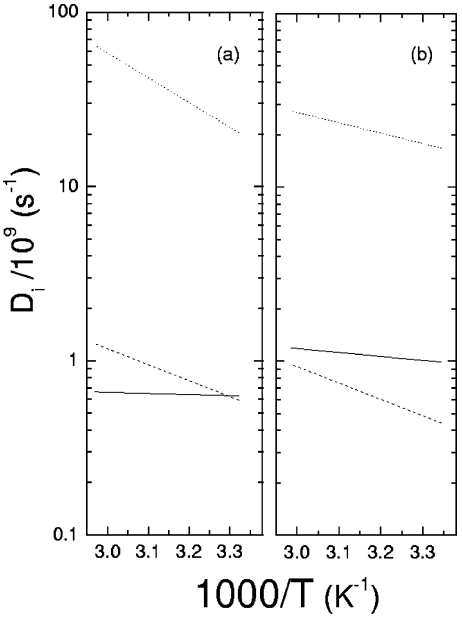

Figure 8. Plots of rotational diffusion coefficients $D_{||}$ (solid line), $D_\perp$ (dashed line), and D' (dotted line) for a 54 (a) and 56 wt % (b) DACl/H_2O sample.

the possibility of finding another motional model (e.g. the cone model[28]) can be envisioned, which could produce more realistic diffusive constants.

Furthermore, relaxation information of C_2/C_3 deuterons has also been examined using the superimposed rotations model. Taking an additional superimposed rotation into account, eq 10 is used to find D'' due to diffusive motions of the C_2/C_3 methylene rotation, while the results of $D_{||}$, $D_\perp$, and D', and their corresponding activation energies $E_{||}^a$, $E_\perp^a$, and E'^a obtained from the above simulation are fixed. However, the similarity of the deuteron relaxation rates for C_1 segment and C_2/C_3 segment suggests that this attempt is doomed to fail. In particular, the fittings were not good and no crossover could be reproduced. Moreover, the diffusion coefficients D'' are smaller for both 54 and 56 wt % samples (4.8×10^9 s^{-1} at 301 K and 7.3×10^9 s^{-1} at 299 K, respectively) in comparison to the corresponding D' (2.0×10^{10} and 1.7×10^{10} s^{-1}). Similarly the activation energy for D'' is also smaller than that for D' in both concentrations (see Table 3). Also it is impossible to fit both J_1 and J_2 of $^2H_{C2}$ with the same D'' value at each temperature. The fact that the three carbon sites relax similarly may suggest that the first few segments of the alkyl chain behave as a "rigid" group, and they share more or less the same internal diffusion parameter. Therefore, the superimposed rotations model is not a suitable model to account for the C_2/C_3 relaxation data. A fully deuterated DACl/H_2O sample is, however, required for testing correlated rotations in the flexible C−C backbone of our system using the decoupled model.[29]

TABLE 2: Fitting Parameters of Rotational Diffusion Coefficients and Their Activation Energies with Error Limits

		54 wt %	56 wt %
preexponential	$D_{||}^\infty$	$(1.02 \pm 0.08) \times 10^9$ s^{-1}	$(5.60 \pm 0.57) \times 10^9$ s^{-1}
	$D_\perp^\infty$	$(5.96 \pm 0.64) \times 10^{11}$ s^{-1}	$(5.73 \pm 0.81) \times 10^{11}$ s^{-1}
	D'^∞	$(9.48 \pm 1.09) \times 10^{14}$ s^{-1}	$(1.57 \pm 0.16) \times 10^{12}$ s^{-1}
activation energies	$E_{||}^a$	1.24 ± 0.20 kJ/mol	4.37 ± 0.27 kJ/mol
	$E_\perp^a$	17.5 ± 0.3 kJ/mol	18.0 ± 0.4 kJ/mol
	E'^a	27.2 ± 0.3 kJ/mol	11.4 ± 0.3 kJ/mol

TABLE 3: Fitting Parameters of Rotational Diffusion Coefficient D'' and Its Activation Energy

	54 wt %	56 wt %
D''^∞	4.78×10^9 s^{-1}	2.43×10^{11} s^{-1}
E''^a	0 kJ/mol	8.7 kJ/mol

5. Conclusion

As another spin one nucleus, ^{14}N NMR not only shares the same theory as ^2H NMR, but also has its own advantage in yielding significant information of molecular dynamics. At the headgroup of DACl-d_{11} molecules, the ^{14}N spin−lattice relaxation measurements in conjunction with those of $^2H_{C1}$ can give us the overall motional information of the DACl molecule in the lamellar phase. The present study also shows that one can gather more reliable information on the location of the long molecular axis for the DACl molecule. Furthermore, the dynamics in the lamellar phase of the studied lyotropic liquid crystal may be treated similar to that of a thermotropic SmA phase, viz., using the small step rotation diffusion model, although $D_\perp$ appears to be comparable to $D_{||}$. This seemingly unrealistic scenario points to a need of further developing a better motional model for lyotropic liquid crystals. In the present study, lower activation energy for the spinning motion than that of the tumbling motion shows that it is relatively easier for molecules to rotate while they are loosely anchored on water. Even though the quadrupolar coupling of ^{14}N nucleus could be relatively large (a few MHz), under suitably motional averaging in lyotropic systems it can be studied by ^{14}N NMR to provide both static and dynamic information. More ^{14}N experiments could be useful to confirm the current work in similar lyotropic systems and to explore improved models to describe molecular dynamics of amphiphilic molecules in lamellar phases.

Acknowledgment. R.Y.D. thanks the Canada Foundation of Innovation, Natural Sciences and Engineering Council of Canada, and Brandon University for their financial support. We thank Dr. A. S. Tracey for allowing us to use his deuterated DACl samples.

References and Notes

(1) Tiddy, G. J. *Phys. Rep*. **1980**, *57*, 1.
(2) Wachowicz, M.; Jurga, S.; Vilfan, M. *Phys. Rev. E* **2004**, *70*, 031701.
(3) Tornblom, M.; Sitnikov, R.; Henriksson, U. *J. Phys. Chem. B* **2000**, *104*, 1529.
(4) Kruger, G. J.; Rademeyer, M.; Billing, D. G. *Acta Crystallogr. E* **2003**, *59*, 0480.
(5) Gorden, M. *Acta Crystallogr*. **1953**, *6*, 739.
(6) Rizzatti M. R.; Gault, J. D. *J. Colloid Interface Sci.* **1986**, *110*, 258.
(7) Fojud, Z.; Szczeniak, E.; Jurga, S.; Stapf, S.; Kimmich, R. *Solid State Nucl. Magn. Reson.* **2004**, *25*, 200.
(8) Quist, P.; Halle, B.; Furo, I. *J. Chem. Phys.* **1991**, *95*, 9.
(9) Dong, R. Y. *Mol. Phys*. **2001**, *99*, 637.
(10) Seliger, J.; Zagar, V.; Blinc, R. *J. Chem. Phys.* **1982**, *78*, 5.
(11) Dong, R. Y.; Tomchuk, E.; Visintainer, J. J.; Bock, E. *Mol. Cryst. Liq. Cryst.* **1976**, 33, 101.
(12) Dong, R. Y. *Chem. Phys. Lett.* **2003**, *375*, 517. Jurga, S.; Macho, V.; Huser, B.; Spiess, H. W. *Z. Phys. B*: *Condens. Matter* **1991**, *84*, 43.
(13) Chen, Y. Molecular Dynamics Study of Liquid Crystals by ^{2}H and ^{14}N NMR Spectroscopy, M.Sc. Thesis, University of Manitoba, 2005.
(14) Wimperis, S. *J. Magn. Reson.* **1990**, *86*, 46.
(15) Charvolin J.; Hendrikx, Y. In *NMR of Liquid Crystals*; Emsley, J. W., Ed.; Reidel: Dordrecht, The Netherlands, 1985.
(16) Jansson, P. L. M. *J. Chem. Phys*. **1989**, *93*, 1448.
(17) Berggren, E.; Tarroni, R.; Zannoni, C. *J. Chem. Phys*. **1993**, *99*, 6180.
(18) Dong, R. Y. *Liq. Cryst*. **1994**, *16*, 1101.
(19) Gustafsson, S.; Halle, B. *Mol. Phys.* **1993**, *80*, 549.
(20) Nordio, P. L.; Busolin, P. *J. Chem. Phys*. **1971**, *55*, 5485.
(21) Tarroni, R.; Zannoni, C. *J. Chem. Phys.* **1991**, *95*, 4550.
(22) Beckmann, P. A.; Emsley, J. W.; Luckhurst, G. R.; Turner, D. L. *Mol. Phys*. **1986**, *59*, 97.
(23) Counsell, C. J. R.; Emsley, J. W.; Heaton, N. J.; Luckhurst, G. R. *Mol. Phys*. **1985**, *54*, 847.
(24) Catalano, D.; Chiezzi, L.; Domenici, V.; Geppi, M.; Veracini, C. A.; Dong, R. Y.; Fodor-Csorba, K. *Macromol. Chem. Phys.* **2002**, *203*, 1594.
(25) Dong, R. Y. *Prog. Nucl. Magn. Reson. Spectrosc*. **2002**, *41*, 115.
(26) Dong, R. Y.; Chen, Y. B.; Veracini, C. A. *Chem. Phys. Lett.* **2005**, *405*, 177.
(27) Press: W. H.; Flannery, B. P.; Teukolsky, S. A.; Vetterlung, N. T. *Numerical Recipes*; Cambridge University Press: Cambridge, UK, 1980.
(28) Dong, R. Y. *NMR of Liquid Crystals*; Springer-Verlag: New York, 1997.
(29) Dong, R. Y. *Phys. Rev. A* **1991**, *43*, 4310.